Journal of
Materials Chemistry B

Accepted Manuscript

This article can be cited before page numbers have been issued, to do this please use: X. Cheng, J. Zhang, H. Chang, F. Nie, L. Luo and X. Feng, *J. Mater. Chem. B*, 2016, DOI: 10.1039/C6TB01158F.

ROYAL SOCIETY OF CHEMISTRY

www.rsc.org/materialsB

View Article Online
DOI: 10.1039/C6TB01158F

Journal of Materials Chemistry B

COMMUNICATION

High Performance Cu/Cu_2O Nanohybrid Electrocatalyst for Nonenzymatic Glucose Detection

Received 00th May 00xx,
Accepted 00th May 00xx

DOI: 10.1039/x0xx00000x

www.rsc.org/

Xiqing Cheng,[ab] Jun Zhang,[b] Hucheng Chang,[b] Liqiang Luo,[a] Fuqiang Nie [b] and Xinjian Feng *[bc]

Here we report Cu/Cu_2O nanocomposites prepared via potential oscillations. High resolution transmission electron microscopy images reveal a homogeneous distribution feature of Cu and Cu_2O in the composite. Due to thesynergistic effect between Cu and Cu_2O, the nanohybrids show much lower resistivity and glucose oxidation activity (lower over-potential and higher current-output) compared to the Cu_2O counterpart. As an example of application, the nanocomposite-based electrode is employed for nonenzymatic glucose biosensor application, which exhibits a linear detection up limit of 40 mM, a sensitivity of 1434.12 μA cm^{-2} mM^{-1}, and good selectivity.

Introduction

The development of high performance electrochemical biosensors has been a subject of extensive research owing to their importance in clinical diagnosis, bioprocess monitoring, and so on.[1-9] Compared to enzyme-based biosensors,[1-6] non-enzymatic sensors can avoid the intrinsic instability of enzyme and the need of electron mediators, has attracted an increasing interests.[7-9] Non-enzymatic biosensors need efficient electrocatalyst for direct substrate oxidization with minimum resistances in electrochemical reaction occurring at electrolyte/electrode interface and the electron conduction in electrode. Among a wide variety of electrocatalysts, nanostructured metal oxides have promising application as nonenzymatic catalysts in biosensors owing to their low cost and high stability, biocompatibility and electrocatalytic activity.[10-19] However, the high resistivity of metal oxides (for example, Cu_2O is 3×10^6 ohm-cm at room temperature)[20] significantly impedes them from wide use in electrochemical biosensor with wide linear detection range, high sensitivity and excellent selectivity.

Integration of metal into the matrix of metal oxide is a novel strategy that can combine the advantages of the catalytic activity of metal oxide and the conductivity of metal. Recently, Cu/Cu_2O composites have been deposited on TiO_2 nanotube arrays via a constant potential approach and applied for nonenzymatic glucose detection. But the linear detection limit is only up to about 2.5 mM.[26] Electrodeposition under conditions of spontaneous potential oscillations is a simple and inexpensive way to prepare nanocomposite of Cu and Cu_2O.[20-23] Materials composing this structure by themselves possess rather interesting optical and electrical properties, however, to the best of our knowledge, there are few reports regarding to their device applications.

Herein, we report the first nonenzymatic biosensor application of Cu/Cu_2O nanocomposite deposited on fluorine doped tin oxide (FTO) coated substrate via potential oscillation for glucose analysis. Such nanohybrid has much lower resistivity and glucose oxidation activity (low over-potential and high current-output) compared to the Cu_2O counterpart. We show that biosensor based on this nanohybrid exhibits a linear detection range of 40 mM, the highest value that has been reported of Cu_2O based devices, and higher than the clinically relevant range (~30 mM).[2] Moreover, the biosensor has a sensitivity of 1434.12 μA cm^{-2} mM^{-1}, good selectivity, and repeatability.

Experimental Section

Chemical: Copper (II) sulfate pentahydrate ($CuSO_4 \cdot 5H_2O$, ⩾ 98.0%), DL-Lactic acid ($C_3H_6O_3$, 90%), were purchased from Sigma (USA). Sodium hydroxide (NaOH, ⩾96.0%), uric acid (UA), ascorbic acid (AA) and Dopamine(DA). All chemicals were directly used without further purification. All solutions were prepared with Milli-Q water except especially mentioned.

[a] Department of Chemistry, College of Science, Shanghai University, Shanghai, 200444, P. R. China
[b] Suzhou Institute of Nano-Tech and Nano-Bionics, Chinese Academy of Sciences, Suzhou, 215123, P. R. China
[c] College of Chemistry, Chemical Engineering and Materials Science, Soochow University, Suzhou 215123, P. R. China. *E-mail: xjfeng@suda.edu.cn

[†]Electronic Supplementary Information (ESI) available: [XRD of Cu_2O, the reproducibility and stability of Cu/Cu_2O modified electrodes]. See DOI: 10.1039/x0xx00000x

View Article Online
DOI: 10.1039/C6TB01158F

Preparation of Cu-Cu_2O and Cu_2O modified electrodes: Prior to the deposition, the FTO (Fluorine-doped Tin Oxide) substrates were rinsed thoroughly with water followed by sonication in acetone, absolute alcohol and water (for 15 min each) in sequence. Finally, the FTO substrates were rinsed thoroughly with water and allowed to dry with nitrogen flow. The electrochemical deposition of Cu/Cu_2O and Cu_2O onto the FTO substrates were conducted in an electrolyte solution consisting of 0.3 M cupric sulfate and 3 M lactic acid. The pH of the electrolyte solution was adjusted to 9 and 13 by the addition of 5 M sodium hydroxide. The Cu/Cu_2O and Cu_2O modified electrodes were fabricated with -0.5 mA/cm^2 and magnetic agitation at room temperature. The saturated calomel electrode (SCE) and a platinum foil served as reference and counter electrodes, respectively.

Apparatus: The morphologies and microstructures of Cu_2O were investigated by using field-emission scanning electron microscope (FE-SEM, HITACHI-S4800, Japan). The transmission electron microscopy (TEM) image were taken using Tecnai F20 (FEI, Hillsboro, OR, USA) microscope at an accelerating voltage of 200 kV. XRD was obtained on a Rigaku DLMAX-2200 X-ray diffractometer using K radiation (λ= 1.5418 Å, 40 kV, 40 mA; scanning rate: 0.2° s^{-1}) in the range of 20-70°. The electrochemical measurements were carried out on a CHI660D electrochemical workstation (Shanghai CH Instrument Co., China). A conventional three-electrode system was used to conduct electrochemical tests consisting of a saturated calomel electrode (SCE) or silver-silver chloride electrode as the reference electrode, a platinum foil as the counter electrode and a modified FTO as the working electrode.

Results and discussion

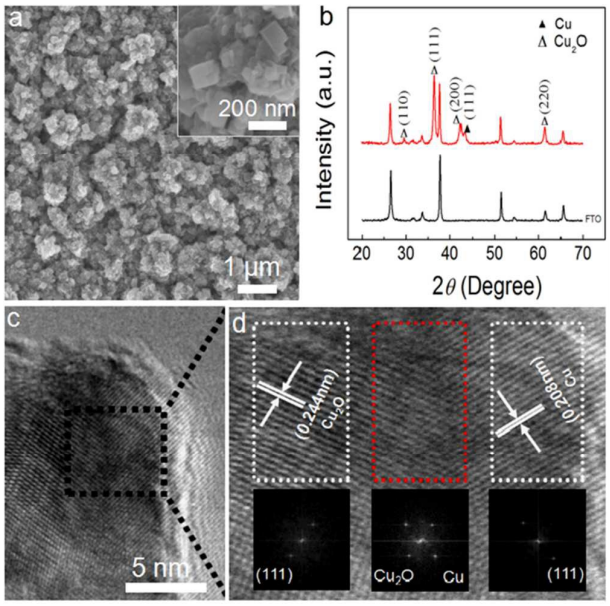

Fig. 1 (a) FE-SEM top view of the Cu/Cu_2O nanohybrid that deposited on FTO substrate. The insert in (a) is a FE-SEM image at higher magnification. (b) XRD pattern of the nanohybrid. Peaks from both Cu and Cu_2O phases were observed. (c) TEM image of part of the nanohybrid. (d) HR-TEM image of the area that marked by black.

In a typical experiment, the nanohybrid is electrodeposited on FTO substrates at a current density of -0.5 mA cm^{-2} using electrolyte of 0.3 M Cu(II) with a pH value of 9. Fig. 1a and the insert are typical field-emission scanning electron microscopy (FE-SEM) top views of the as-deposited electrocatalyst at low and high magnification, respectively. The film is composed of microscale particles that aggregated from cubic nanoparticles with diameter of about 100 nm. Fig. 1b shows the powder X-ray diffraction (XRD) patterns. The peaks at 29.63° , 36.50° , 42.40° and 61.52° can be, respectively, indexed to the (110), (111), (200) and (220) plane of Cu_2O (JCPDS file no: 65-3288). In addition, a relatively weak peak at 43.407° that can be indexed to the (111) plane of Cu (JCPDS file no: 65-9743) is observed. These results confirm that Cu/Cu_2O nanocomposite has been successfully obtained. More detail information on the microstructure of the nanohybrid is gained from high resolution in the left and right parts as marked with white boxes. These d-spacing can be, receptively, indexed to the (111) planes of cubic phase Cu_2O and Cu, which is consistent with their corresponding fast Fourier transform (FFT) patterns shown below. HR-TEM image at their border area as marked with red box in Fig. 1d and its corresponding FFT pattern illustrates lattice fringes of both Cu_2O and Cu. These results indicate that the as-prepared nanohybrid has a good crystallinity and is a homogeneous mixture of metal and metal oxide.

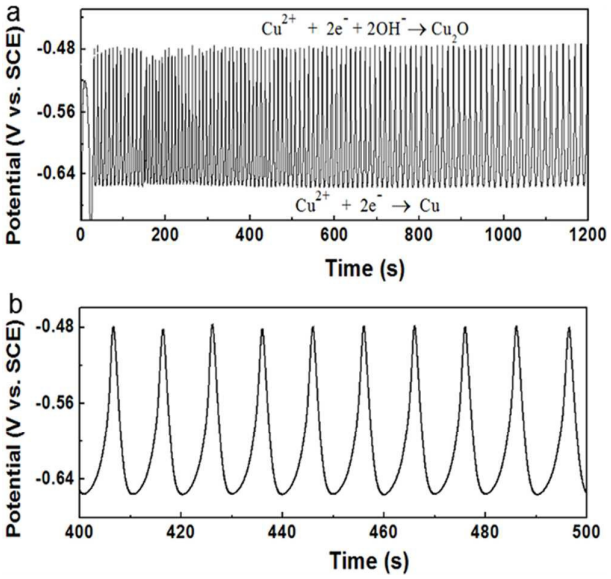

Fig. 2 Potential oscillations recorded during the electrodeposition in electrolyte with pH value of 9. The oscillation persist for hours in a stirred solution.

Fig. 2 shows the electrodeposition curves with a typical potential oscillation feature that recorded when the deposition is carried out in an electrolyte with pH value of 9. The potential oscillates constantly in a stirred solution

View Article Online
DOI: 10.1039/C6TB01158F

between -0.46 and -0.64 V vs. SCE. Such oscillation could be a result of the pH oscillations at the electrode/electrolyte interface during the electrodeposition. When pH value at the electrode/electrolyte interface is high, the formation of Cu_2O is favored ($2Cu^{2+} + 2\ e^- + 2\ OH^- \rightarrow Cu_2O + H_2O$) during the positive-going spike in potential.[20-23] As Cu_2O is deposited, OH^- ions at the electrode surface would be rapidly consumed, but cannot be supplied effectively from the electrolyte due to the slow diffusion rate of OH^- in aqueous solution. This results in the decrease of interface pH value and the deposition of Cu ($Cu^{2+} + 2e^- \rightarrow Cu$), which is thermodynamically favored.[23] During the deposition of Cu, the local pH value would increase following the diffusion of OH^- from the bulk electrolyte, which consequently result in the transition from Cu to Cu_2O deposition and the potential oscillation. In contrast, when the electrodeposition is operated in electrolyte with high pH value, such as 13, no potential oscillation curve is observed and only pure Cu_2O is deposited as shown in Fig. S1 and S2. This can be attributed to the fact that OH^- consumed during Cu_2O deposition can be effectively supplied from bulk solution due to the high diffusion concentration gradient and the high diffusion rate, as a result, no Cu can be deposited. These results indicate that the Cu/Cu_2O nanocomposite are produced only when the potential oscillations are observed.

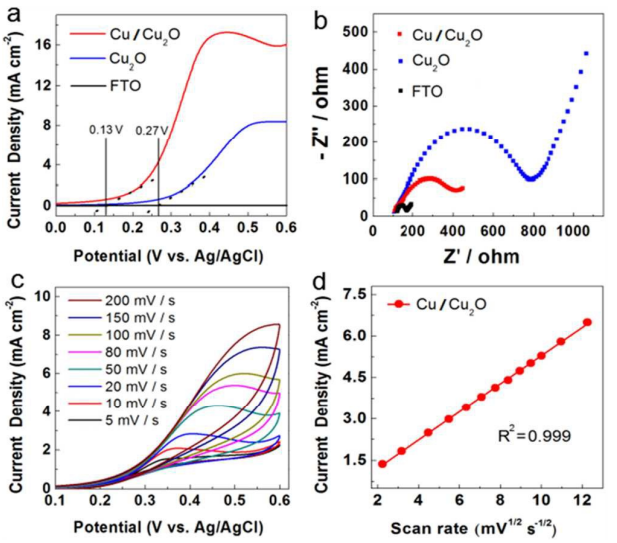

Fig. 3 (a) LSVs of Cu/Cu_2O and Cu_2O that deposited on FTO substrate in electrolyte with pH value of 9 and 13, respectively, in the presence of 10 mM glucose in 0.1 M NaOH (scan rate of 20 mV s^{-1}). (b) EIS recorded in 5.0 mM $[Fe(CN)_6]^{3-/4-}$ + 0.1 M KCl at bare FTO, Cu/Cu_2O and Cu_2O based electrodes. EIS parameters: frequency range of 0.1-10^5 Hz, and 5 mV amplitude of sine voltage signal. (c) CV curves of Cu/Cu_2O based electrode in 1 mM glucose and 0.1 M NaOH solution at different scan rates. (d) Plot of peak currents vs. scan rate $v^{1/2}$.

The electrocatalytic activity of the nanocomposite towards glucose oxidation was further studied. As shown in Fig. 3a, the peak current density of 16.76 mA cm^{-2} was obtained on the Cu/Cu_2O modified electrode, which is 2 times higher than the value achieved on Cu_2O, indicating that the nanohybrids has much higher electro-activity. Negligible current response was observed on bare electrode. We can also see that the oxidation current of the Cu/Cu_2O hybrids starts from about 0.13 V. In contrast, the oxidation current of Cu_2O starts at around 0.27 V, indicating that the oxidation potential shift 140 mV negatively relative to that of Cu_2O after the integration of Cu, which can be attribute to the difference in electron conduction of electrode materials. Electrochemical impedance spectroscopy (EIS) is used to investigate the electron transfer property of electrode materials. As shown in Fig. 3b, the Ret value of Cu/Cu_2O is 173.8 Ω, much lower than the value of Cu_2O (447.3 Ω), indicating that the resistivity of Cu/Cu_2O composites is much lower than that of Cu_2O, which explains the difference in oxidation over-potential of these two electrode materials. Fig. 3c shows the cyclic voltammograms of the Cu/Cu_2O electrode recorded in 1 mM glucose solution at different scan rates in the range of 5 mV s^{-1} to 200 mV s^{-1}. It is found that anodic peak currents increase distinctly with the increasing potential scan rate. The anodic peak currents are linearly correlated to the square root of scan rate (Fig. 3d), implying that the electrode surface oxidation reaction is not electrocatalyst kinetics limited, but instead a typical diffusion-controlled process.

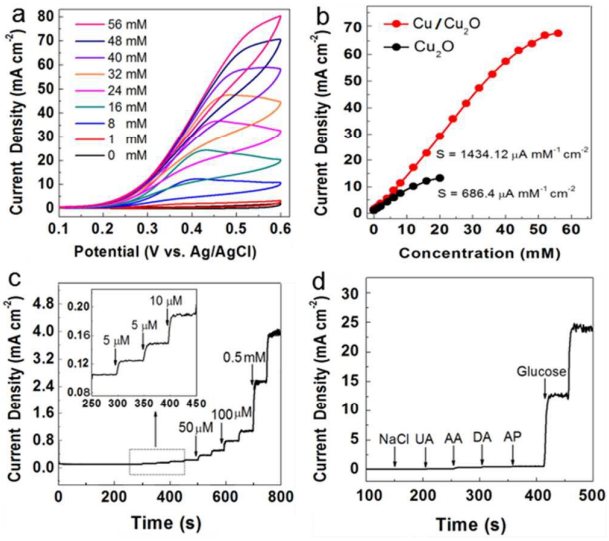

Fig. 4 Performance of Cu/Cu_2O based electrode for non-enzymatic glucose detection. (a) CVs corresponding to the electroxidation of glucose with various concentrations. (b) Calibration plot derived from the CVs at 0.5 V versus SCE. (c) Current-time curves recorded on Cu/Cu_2O electrode upon the addition of different concentrations of glucose at an applied potential of 0.5 V. The detection limit is 1.6 μM. (d) Amperometric responses of Cu/Cu_2O electrode to the successive addition of 0.1 mM NaCl, UA, AA, DA, AP and 5 mM glucose in 0.1 M NaOH electrolyte.

The Cu/Cu_2O nanohybrid with such unique microstructure and electrical property will be of broad academic and industrial interests. In this work, we investigated its application as an electrode in non-enzymatic biosensor for glucose detection, where minimum resistance in electrochemical

View Article Online
DOI: 10.1039/C6TB01158F

reaction occurring at electrolyte/electrode interface and excellent electron conduction in electrode materials are essential for high device performance. CVs (Fig. 4a) show that the electroxidation current increases steadily with the increases of glucose concentration up to a value of 56 mM. From the calibration plot of current versus concentration shown in Fig. 4b (red line), it can be seen that a linear detection range of 40 mM, much higher than the clinically relevant range ~ 30 mM,[2] is achieved. The detection sensitivity is 1434.12 μA cm^{-2} mM^{-1}. In contrast, as illustrated in the insert in Fig. 4b, control experiment based on Cu_2O modified electrode gives linear detection range only up to about 10 mM, similar to the values reported previously based on Cu_2O[17,24,25] and Cu_2O electrochemically deposited on TiO_2 nanotube arrays,[26] but much lower than that achieved on Cu/Cu_2O nanohybrid modified electrode. Fig. 4c shows the detection limit and response time of the Cu/Cu_2O based electrode. The electrode response rapidly within 5s upon the addition of glucose and has a detection limit of 1.6 μM (S/N=3). The results demonstrate the outstanding performance of Cu/Cu_2O nanohybrid based nonenzymatic biosensor.

Selectivity, reproducibility and stability are crucial importance for the practical application of electrochemical biosensor. Fig. 4d shows the performance of Cu/Cu_2O nanohybrid based electrode upon successive addition of 0.1 mM NaCl, uric acid (UA), ascorbic acid (AA), dopamine (DA), acetamidophenol (AP) and 5 mM glucose. There is only a total of 3.3% increase in the current density after the addition of these interferents, suggesting a high selectivity of Cu/Cu_2O electrode for glucose detection. The reproducibility and stability of the electrodes are investigated by cyclic voltammetry (Fig. S3). Results based on five separately fabricated electrodes give a relative standard deviation (RSD) of 4.5% while measuring 10 mM glucose, indicating acceptable reproducibility of the glucose sensor. For the same electrode, the relative standard deviation for 80 times continuous measurements in the presence of 10 mM glucose concentration is calculated to be 3.7%, indicating a good stability and repeatability of the electrode material. In addition, the long-term stability of the sensor is examined by measuring the amperometric response of electrode at every 5-day intervals in the presence of 10 mM glucose. The current remained 90% of its initial values after a month. These results confirm that the proposed Cu/Cu_2O nanohybrid based electrode has a good selectivity, reproducibility and stability.

Conclusions

In summary, we have developed a homogenous nanohybrid of Cu/Cu_2O as a high performance electrode material for non-enzymatic sensor with wide linear detection range, high sensitivity, excellent selectivity and short response time. The nanohybrids modified electrode has a low overpotential and high electrocatalytic activity towards glucose oxidation. Such impressive performance of the nanocomposite and sensing behaviour of the corresponding electrode originate from the homogeneous integration of metal into the metal oxide, which simultaneously minimizes the resistance of electron conduction between electrode material and electrode/electrolyte interface where electrochemical reaction occurs. We believe that the homogenous metal/metal oxide nanohybrids will promise prospects for the development of non-enzymatic biosensor and biofuel cell devices.

Acknowledgements

X. F. acknowledges financial support from the National Natural Science Foundation of China (21371178), the Jiangsu Province Science Foundation for Distinguished Young Scholars (BK20150032), and the Chinese Thousand Youth Talents Program (YZBQF11001). F. N. L. acknowledge the supported from National Natural Science Foundation of China (NOs.21271182, 21301188, and 61571278) and Postdoctoral Research Funding (2014M550794).

Notes and references

1 Y. Xiao, F. Patolsky, E. Katz, J. F. Hainfeld and I. Willner, *Science*, 2003, **299**, 1877-1881.
2 A. Heller and B. Feldman, *Chem. Rev.*, 2008, **108**, 2482-2505.
3 D. Y. Zhai, B. R. Liu, Y. Shi, L. J. Pan, Y. Q. Wang, W. B. Li, R. Zhang and G. H. Yu, *ACS Nano*, 2013, **7**, 3540-3546.
4 C. Z. Zhu, G. H. Yang, H. Li, D. Du and Y. H. Lin, *Anal. Chem.*, 2015, **87**, 230-249.
5 Y. J. Lei, R. Z. Sun, X. C. Zhang, X. J. Feng and L. Jiang, *Adv. Mater*, 2016, **28**, 1477-1481.
6 C. L. Xu, Z. Q. Song, Q. Xiang, J. Jin and X. J. Feng, *Nanoscale*, 2016, **8**, 7391-7395.
7 K. E. Toghill and R. G. Compton, *Int. J. Electrochem. Sci.*, 2010, **5**, 1246-1301.
8 S. Park, H. Boo and T. D. Chung, *Anal. Chim. Acta.,* 2006, **556**, 46-57.
9 P. Si, Y. J. Huang, T. H. Wang and J. M. Ma, *RSC Adv.*, 2013, **3**, 3487-3502.
10 X. Y. Lang, H. Y. Fu, C. Hou, G. F. Han, P. Yang, Y. B. Liu and Q. Jiang, *Nat. Commun.*, 2013, **4**, 2169-2176.
11 F. Xiao, J. B. Song, H. C. Gao, X. L. Zan, R. Xu and H. W. Duan, *ACS Nano*, 2012, **6**, 100-110.
12 X. C. Dong, H. Xu, X. W. Wang, Y. X. Huang, M. B. Chan-Park, H. Zhang, L. H. Wang, W. Huang and P. Chen, *ACS Nano*, 2012, **6**, 3206-3213.
13 J. Lu, I. Do, L. T. Drzal, R. M. Worden and I. Lee, *ACS Nano*, 2008, **2**, 1825-1832.
14 G. M. Wang, X. H. Lu, T. Zhai, Y. C. Ling, H. Y. Wang, Y. X. Tong and Y. Li, *Nanoscale*, 2012, **4**, 3123-3127.
15 C. C. Kong, L. L. Tang, X. Z. Zhang, S. D. Sun, S. C. Yang, X. P. Song and Z. M. Yang, *J. Mater. Chem. A*, 2014, **2**, 7306-7312.
16 C. Q. Dong, H. Zhong, T. Y. Kou, J. Frenzel, G. Eggeler and Z. H. Zhang, *ACS Appl. Mater. Interfaces*, 2015, **7**, 20215-20223.
17 A. R. Chen, Y. Ding, Z. M. Yang and S. C. Yang, *Biosens. Bioelectron.*, 2015, **74**, 967-973.

View Article Online
DOI: 10.1039/C6TB01158F

18 X. M. Liu, Y. M. Sui, X. Y. Yang, L. N. Jiang, F. Wang, Y. J. Wei and B. Zou, *RSC Adv.*, 2015, **5**, 59099-59105.
19 L. Zhang, H. Li, Y. H. Ni, J. Li, K. M. Liao and G. C. Zhao, *Electrochem. Commun.*, 2009, **11**, 812-815.
20 J. A. Switzer, C. J. Hung, L. Y. Huang, F. S. Miller, Y. C. Zhou, E. R. Raub, M. G. Shumsky and E. W. Bohannan, *J. Mater. Res.*, 1998, **13**, 909-916.
21 J. A. Switzer, C. J. Hung, L. Y. Huang, E. R. Switzer, D. R. Kammler, T. D. Golden and E. W. Bohannan, *J. Am. Chem. Soc.*, 1998, **12**0, 3530-3531.
22 J. A. Switzer, C. J. Hung, E. W. Bohannan, M. G. Shumsky, T. D. Golden and D. C. Van Aken, *Adv. Mater.*, 1997, **9**, 334-338.
23 E. W. Bohannan, L. Y. Huang, F. S. Miller, M. G. Shumsky and J. A. Switzer, *Langmuir*, 1999, **15**, 813-818.
24 F. H. Meng, W. Shi, Y. N. Sun, X. Zhu, G. S. Wu, C. Q. Ruan, X. Liu and D. T. Ge, *Biosens. Bioelectron.* 2013, **42**, 141-147.
25 M. Long, L. Tan, H. T. Liu, Z. He and A. D. Tang, *Biosens. Bioelectron.*, 2014, **59**, 243-250.
26 Q. Yang, M. Long, L. Tan, Y. Zhang, J. Ouyang, P. Liu and A. D. Tang, *ACS Appl. Mater. Interfaces*, 2015, **7**, 12719-12730.

View Article Online
DOI: 10.1039/C6TB01158F

TOC

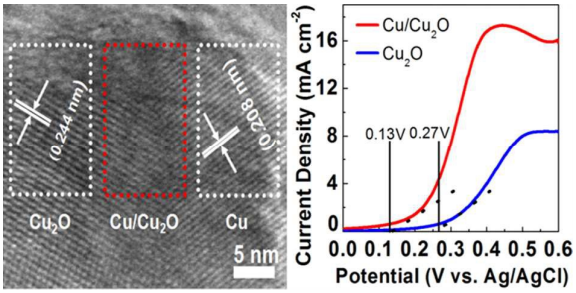

Described herein is Cu/Cu_2O nanohybrids prepared via potential oscillation and their high performance for nonenzymatic glucose detection applications.